

THE ARGONNE TANDEM AS INJECTOR TO A SUPERCONDUCTING LINAC

MASTER

by

J.L. Yntema, P.K. Den Hartog, W. Henning, and W. Kutschera

~~CONFIDENTIAL~~

~~CONFIDENTIAL~~

Prepared for
Fifth Tandem Conference
Catania, Italy
June 9-12, 1980



ARGONNE NATIONAL LABORATORY, ARGONNE, ILLINOIS

**Operated under Contract W-31-109-Eng-38 for the
U. S. DEPARTMENT OF ENERGY**

The submitted manuscript has been authored by a contractor of the U. S. Government under contract No. W31109-ENG-38. Accordingly, the U. S. Government retains a non-exclusive, royalty-free license to publish or reproduce the published form of this contribution, or allow others to do so, for U. S. Government purposes.

THE ARGONNE TANDEM AS INJECTOR TO A SUPERCONDUCTING LINAC

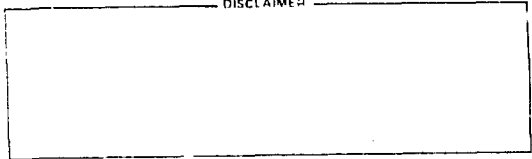
J. L. YNTEMA, P. K. DEN HARTOG, W. HENNING and W. KUTSCHERA

Argonne National Laboratory, Argonne, Illinois 60439*

ABSTRACT

The Argonne Tandem uses Pelletron chains, NEC accelerator tubes, and a dual closed-corona system. Its main function is to be an injector for a superconducting linear accelerator. As long as the transverse and longitudinal emittances are within the acceptance of the linac, the output beam quality of the tandem-linac system is essentially determined by the tandem. The sensitivity of the linac to the longitudinal emittance $\Delta E \Delta t$ of the incident beam makes the output beam quality dependent on the negative-ion velocity distribution in the source, transit-time effects in the tandem, molecular-beam dissociation, and stripper-foil uniformity. This paper discusses these beam-degrading effects.

DISCLAIMER



* Work performed under the auspices of the U.S. Department of Energy.

6215

1. Introduction

To use smaller tandems such as a FN tandem for nuclear physics experiments with heavy ions, it is desirable to post-accelerate the tandem beam. The heavy ion beam of the Argonne FN tandem is post-accelerated with a superconducting linear accelerator¹⁾. The linear accelerator has a modular structure and independently-phased resonators. The sections installed so far have produced acceleration potentials of 11 MV, and additional sections under construction are expected to increase the acceleration potential to at least 20 MV in 1981.

Energetic heavy-ion collisions produce a wide variety of reaction products, the identification of which requires the use of time-of-flight methods. The longitudinal emittance (i.e., the product $\Delta E \Delta t$) of the beam at the exit of the post accelerator is therefore a determining factor in the quality of the experimental data obtainable. The longitudinal emittance $\Delta E \Delta t$ is in essence determined by the tandem. Also, the beam intensity and the constancy of the beam characteristics are important factors determined by the tandem. Thus, a tandem of exceptional quality is essential to the successful operation of a tandem-booster accelerator system.

2. Upgrading of the ANL tandem

In 1973, the belt charging system of the Argonne FN tandem was changed to two Pelletron chains. The total upcharge available from the chains is about 160 μA . This relatively small upcharge current made it desirable to change the voltage-distribution system along the column from resistors to a corona system. The corona system is a closed system which is independently pressurized with SF_6 . The pressure in the corona system is adjusted so that for a given terminal voltage, the current through the corona tubes is about 25 μA . The installation of the chains and corona system

resulted in decreased terminal-voltage fluctuations — typically 400 V peak to peak — and increased voltage-holding capability through the use of somewhat higher SF₆ pressures. With HVEC inclined field tubes, experimental data were taken at terminal voltages as high as 9.75 MV.

In 1977, the inclined field tubes were replaced by the axially symmetric NEC tubes. Since the HVEC column modulus differs from the one of the NEC accelerator tubes, it is necessary to have both a column and an accelerator-tube voltage-distribution system. The accelerator-tube corona system is also an independently-pressurized closed-corona system. The accelerator-tube assembly is attached to the column structure at every eighth column plane. The FN structure allows the installation of 24 accelerator-tube sections in both the high-energy and low-energy sides of the machine. This results, if one uses the nominal 333-kV/section gradient, in a 8-MV machine. In practice, the machine runs well at 9 MV.

Since axially-produced electrons are not adequately suppressed in this accelerator-tube structure, permanent magnets and an electron trap are installed in the dead sections halfway between the base of the tandem and the terminal. This substantially eliminates the x-ray flux which might result from a 9-MeV electron beam.

The vacuum in the accelerator tubes and terminal is typically in the low 10⁻⁸ Torr range. The accelerator tubes do not show pronounced deconditioning effects, provided all traces of moisture in the accelerator tubes are carefully avoided.

To reduce the lens effect of the low-energy accelerator tube, the gap in the column corona system for the first 8 planes is about half the gap in the remaining planes. The first accelerator tube has a corona system which distributes the voltage between the odd numbered accelerating electrodes. To

avoid excessive voltage drifts on the floating even-numbered accelerating electrodes, an open-corona needle assembly is attached to each plane.

Whereas the lifetime of the needles in the corona systems as a whole at this time exceeds 15,000 hours, the special assembly associated with the entrance lens may require more frequent replacement. The needle erosion caused by use changes the voltage distribution in such a way as to increase the lens strength of the entrance to the accelerator tube. This results in a decrease of the transmission of heavy-ion beams. Negative-ion currents of $3 \mu\text{a}$ of ^{32}S have been accelerated with a transmission of about 60%. The transmission for similar beams after 10,000 hours of operation had decreased to about 25%. Replacing the corona needles at the entrance to the accelerator restored the transmission to its original value.

3. The tandem-linac system

A schematic diagram of the Tandem-Linac system is shown in fig. 1. The negative-ion beam is injected into the tandem at an energy of about 135 kV, bunched by the harmonic pretandem buncher²⁾, and foil stripped in the terminal. The beam is focussed on the object slits of a 90° analyzing magnet and rebunched by Buncher 2. The second stripper can be placed either just after the object slits of the magnet (as shown by Stripper #2) or at the time focus in front of the Linac (as shown by Stripper #3).

The pretandem buncher²⁾ compresses about 75% of the ion-source beam into pulses which are approximately 1 ns wide with a frequency of 48.5 MHz. Prior to injection into the linear accelerator, this beam is rebunched by a superconducting resonator (Buncher 2) to a width of less than 100 ps. A phase detector³⁾ next to the superconducting buncher senses the actual beam pulse arrival time and corrects slow drifts in transit time through the accelerator.

A major contribution to the width of the tandem beam pulse arises from the differences in path length of ions through the 90° magnetic analyzer. This magnet has a mass \times energy product of 52, inadequate for the bending of the most probable charge states of ^{58}Ni . To increase the mass \times energy product of the analyzer without changes in the location of either the tandem or the linac and without building modifications, an isochronic superconducting magnetic analyzer⁴⁾ consisting of two 45° magnets with a mass \times energy product of 400 is being designed. With this system, the path-length differences between ions will be largely eliminated. The major effects in time spreads Δt will then be caused by the prebuncher and by the energy spread in the beam at buncher 1.

4. Tandem injection

Figure 2 is a schematic diagram of the tandem injection system. This system should produce a waist of less than 3 mm radius both in the x and y planes about 40 cm in front of the accelerator tube. The heavy-ion source is an inverted sputter source⁵⁾ with a distributed extraction potential⁶⁾ and an extraction einzel lens assembly. Ions are accelerated with two NEC accelerator tubes and refocused by a second einzel lens prior to mass analysis by a 40° double-focussing magnet with a mass \times energy product of 20. The beam is then focussed to the entrance waist by an electrostatic quadrupole triplet lens. If one were to use an einzel lens instead of a quadrupole triplet at this point, it would not be possible to produce the waists in the x plane and y plane at the same distance from the accelerator-tube entrance and, consequently, additional large losses in transmission would result.

A schematic view of the injection optics is shown in fig. 3. The time spread of the beam bunched by the pretandem buncher is due mostly to

the flight path differences through the 90° magnet and to some extent to the deviations of the buncher wave form from the sawtooth. However, if the energy spread of the ions at the buncher exceeds about 30 eV at the nominal injection energy of 132 kV, the energy spread of the ion beam can become the determining factor for the time spread.

The energy spread of ions from the sputter source is normally about 7 eV FWHM. However, Doucas⁷⁾ has shown that much wider energy distributions do occur. Such wider distributions are especially frequent for O⁻ beams, and we experienced one instance in which the source produced a component which, at the end of the linac, was several hundreds keV higher than the main O beam.

The power supply for the preacceleration system has proven to be critically important. The Argonne tandem uses a 150-kV Deltatron Supply⁸⁾ with a ripple and stability of 0.002% or better.

5. Foil stripping

The configuration of the terminal of the FN tandem makes it difficult to use gas stripping while retaining a vacuum of about 10^{-7} Torr in the accelerator tubes near the terminal. Consequently, the system has operated exclusively with foil stripping. The NEC foil stripper has 230 foil positions and, therefore, fairly frequent reloading is necessary. Experimentally, it was found that venting of the accelerator tubes is undesirable. Therefore, all-metal valves similar to the ones developed at the Australian National University⁹⁾ have been installed at either side of the foil stripper, using the electron-trap apertures as one of the sealing surfaces. After a foil change, the terminal is pumped down to a pressure of about 3×10^{-7} Torr prior to the opening of these valves. Under these conditions, the total interruption for a foil reloading is about 36 hours when the tandem is operated at a terminal voltage of 8.6 MV.

The lifetime of the foils becomes a serious problem when the required beam intensities increase and when the post acceleration of ions heavier than Ca becomes feasible. The homogeneity of the foils and their thickness are the dominant factors determining the energy spread ΔE of the tandem beam. The present picosecond bunching system allows one to measure the energy straggling produced by the stripper foils. In this application, the amplitude of the superconducting buncher is adjusted to produce a time focus in a scattering chamber approximately 17 m downstream, where the time width of the beam pulse is measured with a silicon surface-barrier detector by detecting ions scattered from a thin gold foil. Due to the inherent, time-uncorrelated energy spread ΔE of the beam pulse, the width of the time pulse will drift apart over the long flight path and, since it depends approximately linearly on ΔE , the energy spread can be determined from the measured time width. The intrinsic time resolution of the detector system, plus potential time drifts in the injected beam pulse place, were measured by turning off the regular superconducting buncher and using the last resonator in the linac as a buncher, with now a much shorter flight path (≈ 4 m) and corresponding much reduced broadening of the time pulse. The measured intrinsic time resolution is ≈ 48 psec.

A time spectrum for the beam from a $5\text{-}\mu\text{g}/\text{cm}^2$ wrinkled C foil is shown in fig. 4 together with the resolution of the detection system. The $5\text{-}\mu\text{g}/\text{cm}^2$ wrinkled C foil was mounted on an annealed Al ring which was then compressed to 93% of its original diameter. The energy straggling of a $5\text{-}\mu\text{g}/\text{cm}^2$ wrinkled C foil is about equivalent to that of a normal $8\text{-}\mu\text{g}/\text{cm}^2$ carbon foil. Similarly wrinkled $3\text{-}\mu\text{g}/\text{cm}^2$ carbon foils are about equivalent to $5\text{-}\mu\text{g}/\text{cm}^2$ normal foils. The lifetime of wrinkled $3\text{-}\mu\text{g}/\text{cm}^2$ carbon foils is compared to that of normal $5\text{-}\mu\text{g}/\text{cm}^2$ carbon foils in fig. 5. The ordinate gives the ratio in charge nanoamperes of the analyzed Ni^{10+} beam to the injected Ni^- beam,

and the abscissa gives the number of incident Ni atoms in nA-hr. The normal foils show an abrupt disintegration of the foils after about 100 nA-hr. While the wrinkled $3\text{-}\mu\text{g}/\text{cm}^2$ foils show fairly constant transmission up to 300 nA-hr, (a transmission about the same as the one observed for the $5\text{-}\mu\text{g}/\text{cm}^2$ non-wrinkled carbon foils), subsequently, a slow but steady decrease in transmission is observed. After 1500 nA-hr, one of the foils appeared to have become a $25\text{-}\mu\text{g}/\text{cm}^2$ thick carbon foil. The charge-state distribution of a ^{32}S beam did not show any deviation from the normal charge-state distribution observed with thin foils. The origin of the foil thickening is not understood. The introduction of a 25-l/sec ion pump in the terminal in order to continuously pump the terminal box during operation did not significantly affect the foil-thickening process. This makes it unlikely that the apparent foil thickening is due to the cracking of residual hydrocarbon vapor in the terminal.

Since gas stripping is not available, Coulomb-explosion effects limit effectively the useful beams to negative single atoms or hydrides.

6. Linac injection

The optical considerations in the coupling of the tandem to the linac place restrictions on the spot size of the tandem beam at the object slits of the analyzing magnet. The tandem beam is focussed at the object slits of the 90° magnet to a width of 0.6 mm. Since the linac prefers an approximately circular beam at its entrance waist, the vertical slits are normally set at 3.5 mm. These dimensions are determined by the need to retain a sufficient constant tandem energy and a sufficient divergence in the y plane to make waist to waist transfer feasible. The problem for the tandem is the need to have extremely good directional stability. This directional stability is necessary to produce a constant analyzed beam energy and a constant arrival

time at the linac entrance which is some distance away from the phase detectors and to produce the reasonably uniform beam intensity needed for coincidence experiments.

Both the beam direction and its transit time are affected by the voltage distribution along the accelerator tube even if the terminal voltage is constant. Changes of beam transit times at constant terminal voltage of as much as 4 ns have been observed when the current through the accelerator corona tubes was changed from 10 μ a to 30 μ a. Similarly, directional effects can be observed in spite of the fact that the accelerator system is in principle axially symmetric. The small deviations from perpendicularity of individual electrodes and, more importantly, of the apertures between tube sections would cancel out but for the fact that the beam is accelerated. It is therefore desirable to keep the pressure in the corona tubes constant and to recirculate the SF₆ gas through purifiers to avoid possible changes in gas resistivity due to breakdown products in the gas.

The second stripper is desirable to produce higher charge states and consequently acceleration to higher energies through the linac. Until now, the second stripper has been located at the object slits of the 90° magnet. It is sometimes difficult to fully separate adjacent doubly-stripped ions with the 90° magnet, since the magnetic rigidity is proportional to $\sqrt{1 + q_1}/q_2$ (q_1 and q_2 are the charge states at the terminal stripper and post stripper, respectively). This leads to a clustering of beam components with a fixed charge state difference $q_2 - q_1$. However, it is more advantageous for heavy ions to have the stripper in position 3 at the time and space waist at the entrance to the linac and perform the charge state separation after the post-acceleration, since one then deals only with higher charge states produced by a single charge state from the tandem.

7. Ion beams

The beam intensities of various beams which are normally available at the tandem are listed in Table I. In some cases, these intensities are limited by an unwillingness to change stripper foils too often.

REFERENCES

- 1) K. W. Shepard, IEEE Trans. Nucl. Sci. NS-26 (1979) 3659. L. M. Bollinger, Proc. Symposium on Heavy Ion Physics From 10 to 200 MeV, Brookhaven National Laboratory Report BNL51 1115, Vol. 2, p. 589.
- 2) F. J. Lynch, R. N. Lewis, L. M. Bollinger, W. Henning and O. D. Deshe, Nucl. Instrum. Methods 159 (1979) 245.
- 3) R. N. Lewis, Nucl. Instrum. Methods 151 (1978) 371.
- 4) R. P. Smith, L. M. Bollinger, J. R. Erskine, L. Genens and J. Hoffman, to be published.
- 5) K. R. Chapman, IEEE Trans. Nucl. Sci. NS-23 (1976) 1109.
- 6) P. J. Billquist and J. L. Ynema, to be published.
- 7) G. Doucas, Int. J. of Mass Spectrometry and Ion Phys. 25 (1977) 71.
- 8) Manufactured by Deltaray Division, High Voltage Eng. Corp., Burlington, Massachusetts, USA.
- 9) D. Weiser, private communication.

TABLE I

Ion beams available from ANL tandem.

Ion	q	Analyzed Beam in nA
^3He	2^+	75 ^a
^4He	2^+	100
^6Li	3^+	300 ^a
^7Li	3^+	600
^9Be	4^+	200
^{10}B	4^+	200 ^a
^{11}B	4^+	200 ^a
^{12}C	5^+	2000
^{13}C	5^+	500 ^a
^{16}O	6^+	3000
^{18}O	6^+	1000 ^a
^{19}F	7^+	1000
^{24}Mg	7^+	200
^{27}Al	7^+	100
^{28}Si	8^+	1000 ^b
^{29}Si	8^+	100
^{30}Si	8^+	100
^{31}P	8^+	200
^{32}S	8^+	1000 ^b
^{34}S	8^+	340
^{35}Cl	9^+	1000 ^b
^{37}Cl	9^+	500
^{40}Ca	9^+	300
^{56}Fe	10^+	500
^{58}Ni	10^+	500 ^b
^{60}Ni	10^+	300 ^b
^{64}Ni	10^+	300 ^a
^{63}Cu	10^+	500 ^b
^{65}Cu	10^+	500 ^b

^aEnriched source material.^bLimited by lifetime of stripper foil.

FIGURE CAPTIONS

- Figure 1. Schematic arrangement of Argonne Tandem and Linac.
- Figure 2. Low energy beam line elements.
- Figure 3. Ion optics for 150 kV injection into the Argonne tandem. S = sputter source, L_1 = source einzel lens, A_1 , A_2 , A_3 = acceleration tubes, W_1 = object waist for 40° analyzing magnet, L_2 = injection einzel lens, M = 40° magnet, B = harmonic buncher, QT = quadrupole triplet lens, W_2 = object waist for the accelerator, AE = low energy accelerator tube entrance.
- Figure 4. Energy straggling measurement of a wrinkled $5\text{-}\mu\text{g}/\text{cm}^2$ carbon foil together with the measurement of the system resolution.
- Figure 5. Lifetime of carbon foils in the tandem terminal under Ni bombardment.

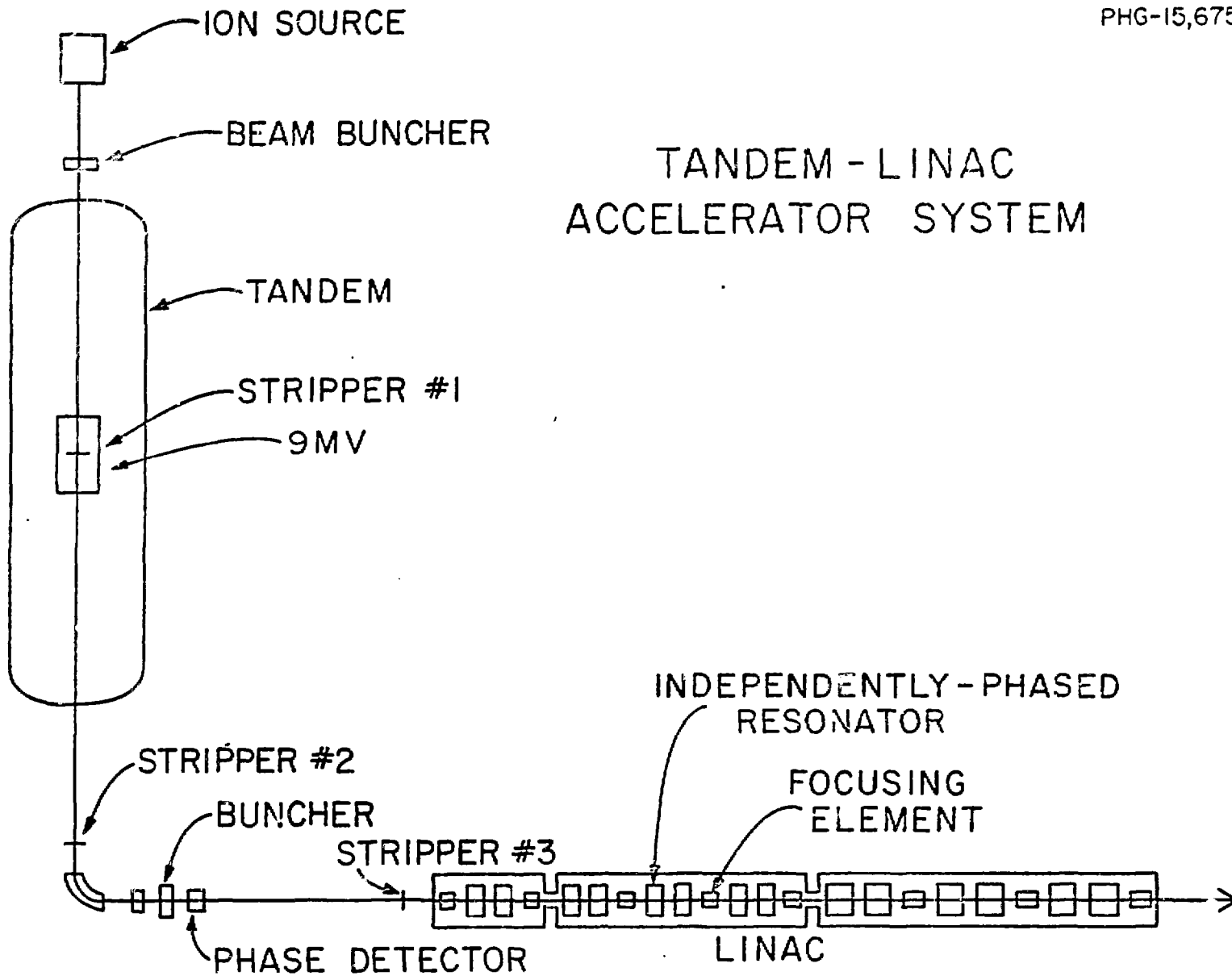


Figure 1

LOW ENERGY BEAM LINE

PHG-14,445

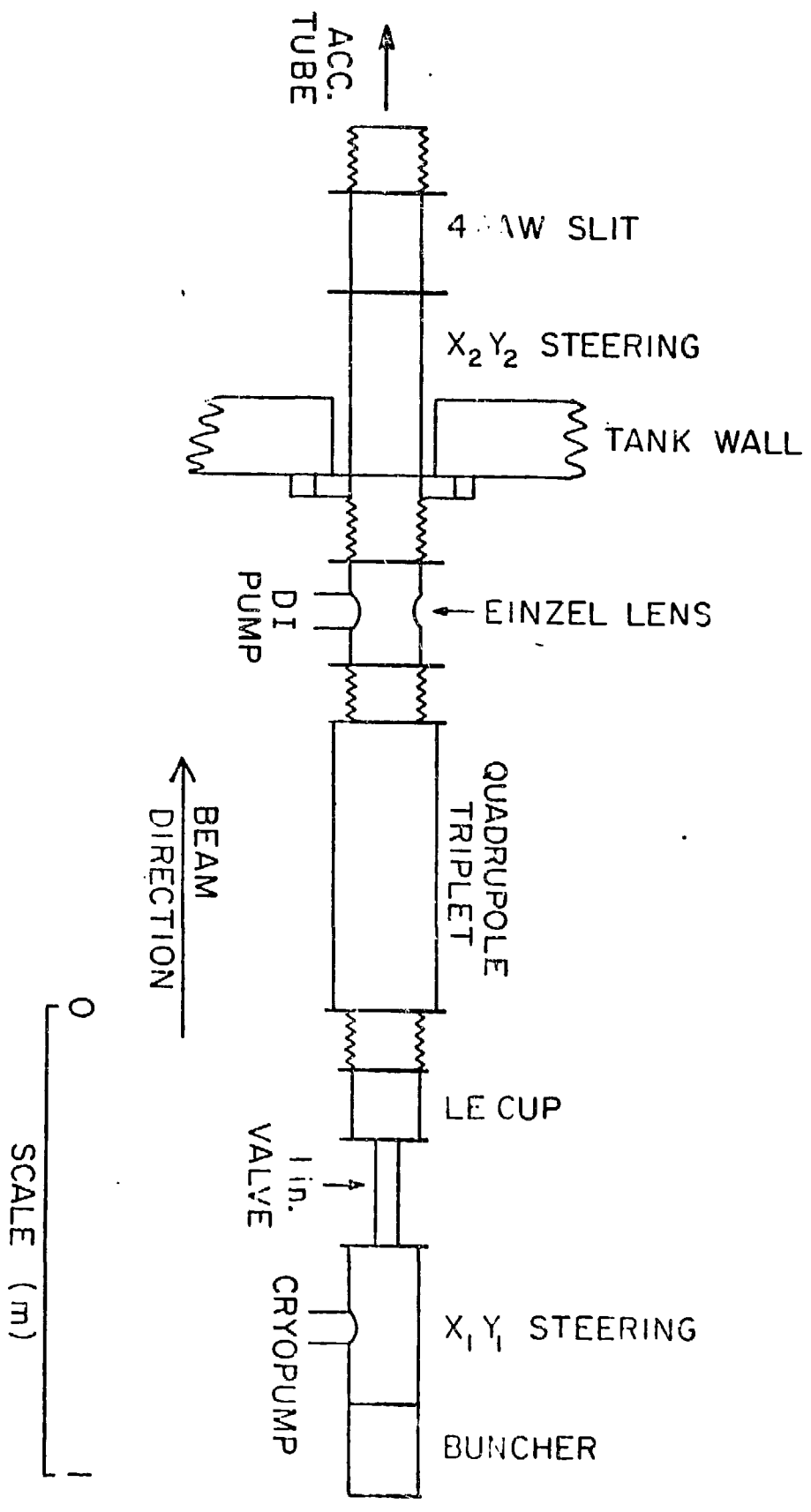


Figure 2

150 KV INJECTION
ARGONNE TANDEM

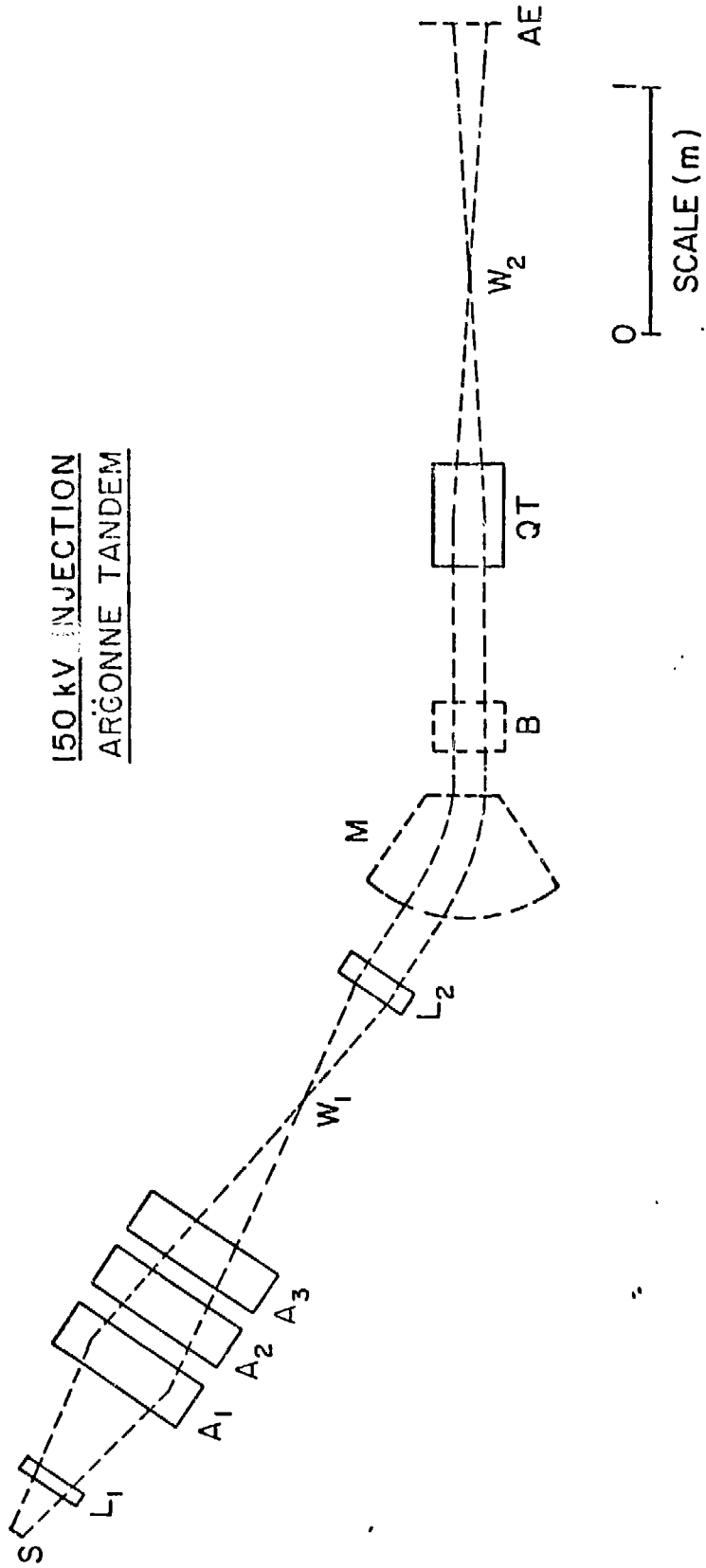


Figure 3

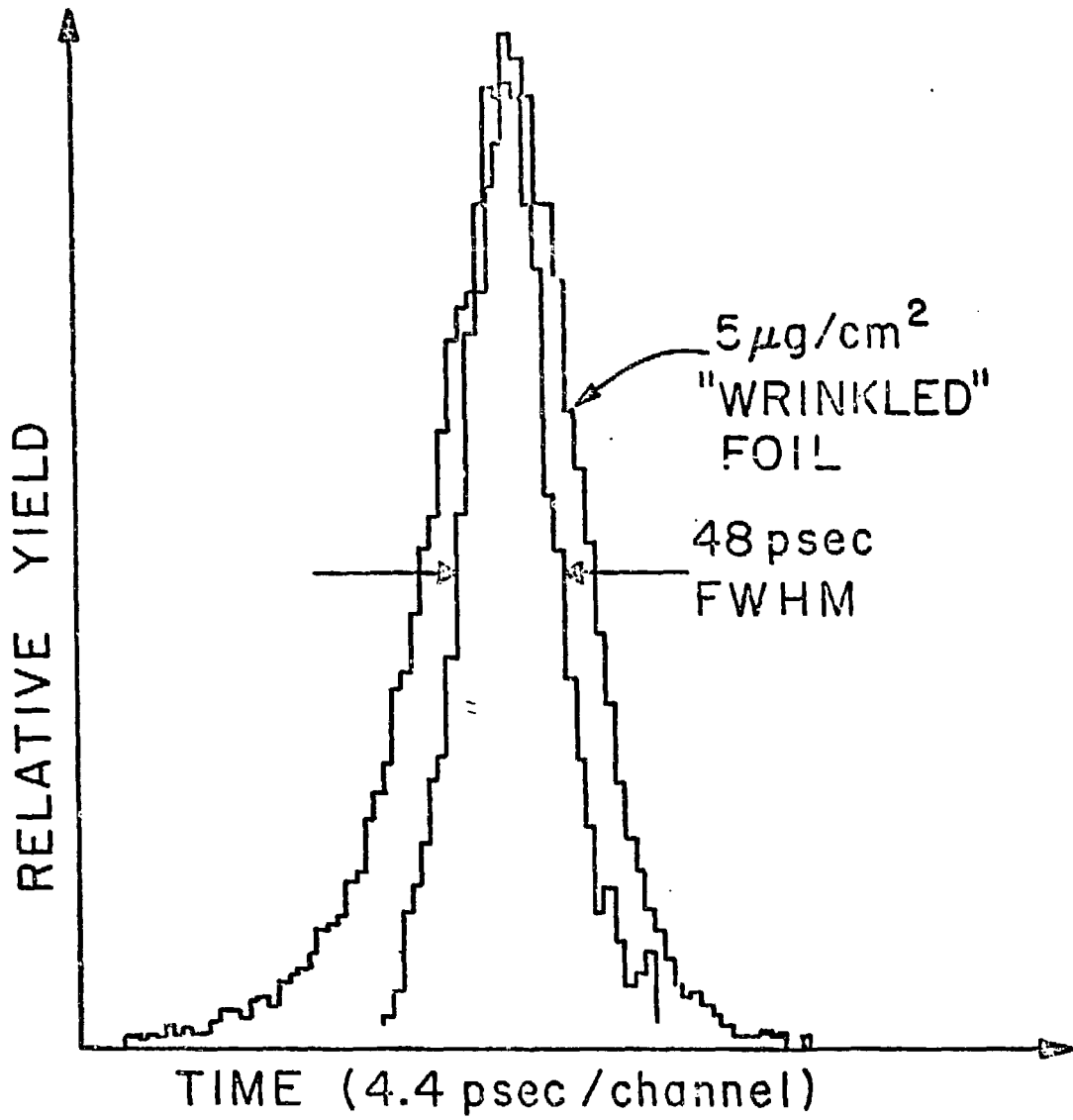


Figure 4

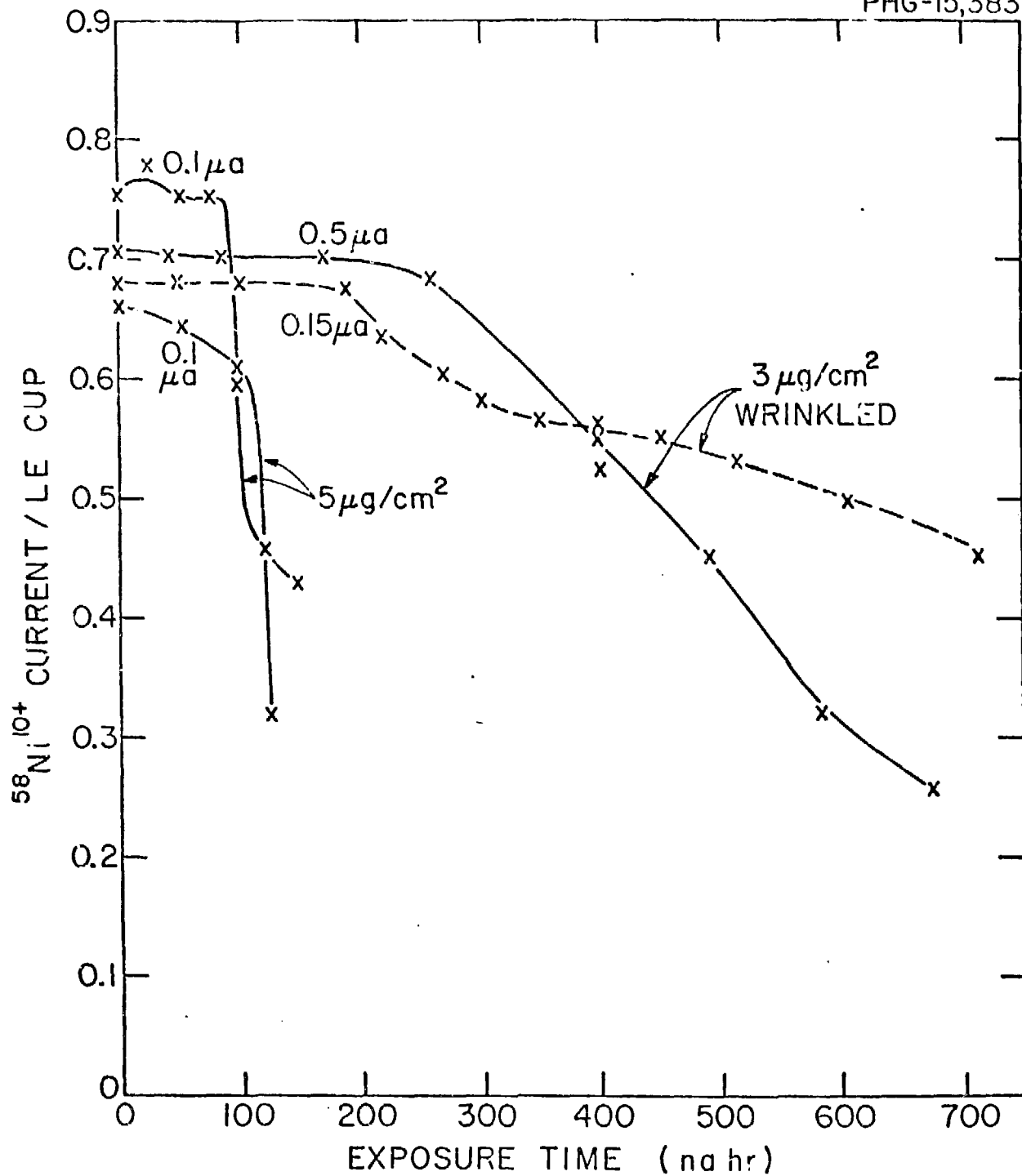


Figure 5